DOI: 10.1002/anie.201201452

Graphene

Linking Photo- and Redoxactive Phthalocyanines Covalently to Graphene**

Maria-Eleni Ragoussi, Jenny Malig, Georgios Katsukis, Benjamin Butz, Erdmann Spiecker, Gema de la Torre, Tomás Torres,* and Dirk M. Guldi**

Dedicated to Professor François Diederich on the occasion of his 60th birthday

Graphene has attracted extensive attention in recent years because of its striking mechanical, optical, and electrical features.[1] This single-atom-thick material is a gapless semiconductor and exhibits electron mobilities reaching values of up to 10 000 $cm^2 V^{-1} s^{-1}$ at room temperature.[2] In fact, this is the basis for a myriad of applications,[3] especially in the area of photovoltaics,[4] either in the form of a transparent conducting electrode[5] or an active component in combination with appropriate organic counterparts such as conjugated polymers.[6] Covalent or non-covalent functionalization of visible-light harvesters/electron donors to graphene has evolved into a promising platform for novel solar cell applications. In this context, there have been a number of articles describing the preparation of graphene/porphyrin nanohybrids.[7] Phthalocyanines (Pcs) are also ideal for this purpose given their outstanding electronic properties and their high absorption coefficients in an important part of the solar spectrum.[8]

A fair amount of work focuses on the non-covalent[9] and covalent[10] functionalization of graphene as a means to overcome the obstacles of low solubility and rather poor processability in virtually any kind of solvent. A leading example is the exfoliation/functionalization of graphite flakes through oxidation reactions [i.e., graphene oxide (GO)], subsequent chemical modification, and, ultimately, reduction to obtain single-layer, functionalized graphene [i.e., reduced graphene oxide (rGO)]. One of the major disadvantages of this procedure is the modification of the intrinsic electronic properties of graphene. In stark contrast, the liquid-phase exfoliation of graphite, namely mild sonication in solvents such as *N*-methylpyrrolidone (NMP), has recently attracted a great deal of attention as a means to obtain stable dispersions of single- or few-layered graphene, which can be further chemically modified.[11]

So far, only two different approaches regarding graphene, that is chemically modified with Pcs, have been established. Firstly, an approach based on the non-covalent functionalization, either between rGO and unsubstituted Pcs[12] or between strongly interacting exfoliated graphene and poly-*para*-phenylenevinylene oligomers containing lateral Pcs.[13] Secondly, an approach, in which GO is employed as starting material for the covalent functionalization with appropriately functionalized Pcs.[14] However, the covalent linkage of Pcs to non-modified graphene obtained by liquid-phase exfoliation of graphite has, to the best of our knowledge, never been reported. In light of the aforementioned, we describe herein the first covalent nanoconjugate, graphene–Pc, using liquid-phase exfoliated graphite. Implicit is that the electronic properties of the covalent graphene–Pc nanoconjugates are somewhat modified. Nevertheless, covalent functionalization of graphene with Pcs offers key advantages such as greater stability of the hybrid material, control over the degree of functionalization, and reproducibility. All of the aforementioned are essential prerequisites for a credible application in solar energy conversion.

Few-layered graphene dispersion was obtained by mildly sonicating graphite flakes in NMP.[11] Covalent functionalization of the above with Pcs was achieved in two steps (Scheme 1). First, 1,3-dipolar cycloaddition of the exfoliated graphite in the presence of an excess of *N*-methylglycine and 4-formylbenzoic acid afforded modified graphene **2**, which bears pyrrolidine rings with pendant phenylcarboxylic acids. Secondly, the esterification reaction between **2** and the alcohol-terminated Pc **1**[15] in the presence of EDC/HOBt yielded graphene-Pc nanoconjugate **3**. The novel graphene-based material **3** and its precursor **2** were thoroughly washed with different solvents to remove molecular aggregates. Notably, **3** forms stable suspensions in solvents such as NMP and DMF (see Figure S1 in the Supporting Information).

[*] Dr. M.-E. Ragoussi, Dr. G. de la Torre, Prof. T. Torres
Departamento de Química Orgánica, Universidad Autónoma de Madrid Cantoblanco, 28049 Madrid (Spain)
E-mail: tomas.torres@uam.es
Homepage: http://www.uam.es/phthalocyanines
J. Malig, G. Katsukis, Prof. D. M. Guldi
Department of Chemistry and Pharmacy and Interdisciplinary Center for Molecular Materials (ICMM), Friedrich-Alexander-Universität Erlangen-Nürnberg, 91058 Erlangen (Germany)
E-mail: guldi@chemie.uni-erlangen.de
Homepage: http://www.chemie.uni-erlangen.de/dcp/assets/pdf/
Dr. B. Butz, Prof. E. Spiecker
Center for Nanoanalysis and Electron Microscopy (CENEM)
Universität Erlangen-Nürnberg, 91058 Erlangen (Germany)
Prof. T. Torres
IMDEA-Nanociencia, c/Faraday 9
Campus de Cantoblanco, 28049 Madrid (Spain)

[**] Financial support from the MICINN and MEC, Spain (CTQ-2011-24187/BQU, PIB2010US-00652), CONSOLIDER-INGENIO (2010 CDS 2007-00010), Nanociencia Molecular (PLE2009-0070), CAM (MADRISOLAR-2, S2009/PPQ/1533), the Deutsche Forschungsgemeinschaft (SFB 583 and FCI), and Cluster of Excellence "Engineering of Advanced Materials (EAM)" is acknowledged.

Supporting information for this article is available on the WWW under http://dx.doi.org/10.1002/anie.201201452.

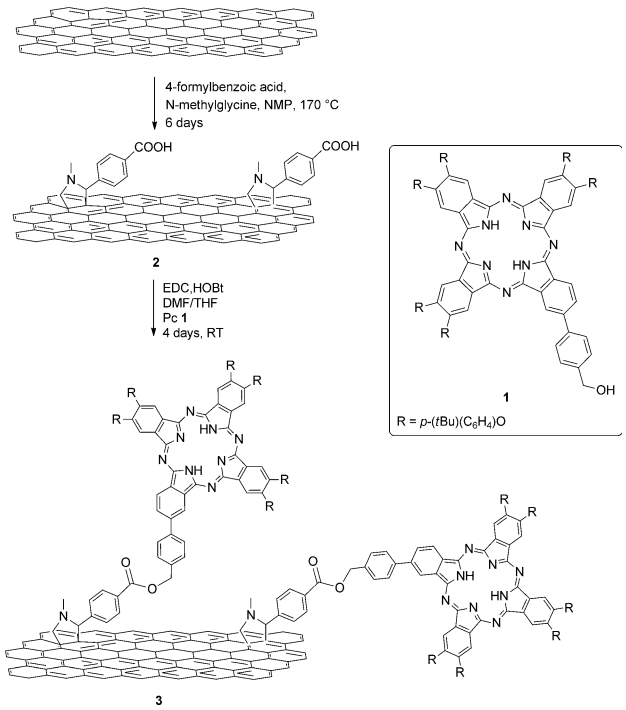

Scheme 1. Synthetic route towards the graphene–Pc nanoconjugate **3**. DMF = N,N′-dimethylformamide, EDC = 1-ethyl-3-(3-dimethylaminopropyl)carbodiimide, HOBt = 1-hydroxybenzotriazole, RT = room temperature, THF = tetrahydrofuran.

The resulting nanoconjugates **2** and **3** were characterized by a number of analytical techniques, such as thermogravimetric analysis (TGA), Fourier transform infrared spectroscopy (FTIR), atomic force microcopy (AFM), transmission electron microscopy (TEM), Raman, as well as steady-state and time-resolved spectroscopic techniques.

The first evidence in support of the successful covalent functionalization of graphene with Pcs is deduced from thermogravimetric analysis. Figure 1 shows the thermal behavior of **3** together with that of **2**, **1**, and pure graphite. The thermogram of **2** shows a weight loss of around 7% at 700 °C, which excludes initial weight losses resulting from

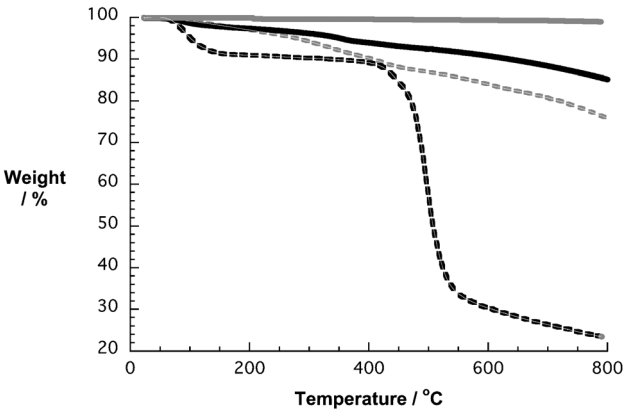

Figure 1. TGA curves of graphite (grey line), graphene nanoconjugate **2** (black line), graphene nanoconjugate **3** (dashed grey line), and Pc **1** (dashed black line) recorded under inert conditions.

adsorbants. For **3**, the thermogram shows an additional 4% weight loss at this temperature, and is directly related to the decomposition of the Pc molecules. Considering that the thermogram of Pc **1** gives rise to an overall decomposition of ca. 65% at 700 °C, the actual weight loss, that is due to covalently attached Pcs, is around 6.5% in **3**. As a matter of fact, the number of Pcs attached to the basal plane of graphene is approximately 1 per 1600 carbon atoms. Overall, the low degree of functionalization is beneficial, since extended patches of undisturbed graphene with its unique electronic features are preserved.

In control experiments a mixture of non-functionalized, exfoliated graphite and Pc **1** were stirred in THF for 4 days, filtered, and washed with several solvents. The thermogram of the resulting graphene material shows no significant weight loss in the 400 to 700 °C regime. As a matter of fact, this finding supports the notion that the weight loss in **3** is exclusively due to covalently attached groups. Additionally, we have hydrolyzed the ester linkage by treating **3** with diluted NaOH in THF under reflux. After 10 h, the absorption spectrum lacks any of the typical Pc characteristics (i.e., Q-band absorption), and the TGA matches that of the graphene precursor **2** (see Figure S2 in the Supporting Information).

FTIR results, as gathered in Figure S3 in the Supporting Information, additionally corroborate the covalent attachment of Pcs to the basal plane of graphene. Notably, the low degree of functionalization of **2** and **3** leads to rather weak signatures in the IR spectra. Nevertheless, a shoulder at around 1710 cm^{-1} is discernable in the FTIR of the precursor **2**, and is assigned to C=O stretch vibrations of the COOH groups. On the other hand, **3** gives rise to an IR feature at around 1730 cm^{-1}, which is likely to relate to C=O stretch vibrations of the ester groups. All of the remaining features are in agreement with those noted for **1**.

Additional insights into the structural features of **3** were gathered from AFM and TEM measurements. AFM images, as illustrated in Figure 2, reveal the presence of few-layer graphene flakes with an average height of approximately 4 nm. AFM thicknesses of our pyrrolidine-modified graphene layers are in line with previous reports (i.e., around 1.5 nm) and clearly evidences the strongly exfoliated character of both **2** and **3**.[16]

Figure 3, and Figures S4 and S5 in the Supporting Information show several TEM and HRTEM images of DMF dispersed **2** and **3**, drop casted onto a lacey carbon grid. The images confirm the coexistence of a partly turbostratic (moiré patterns are visible, Figure S5) and regularly stacked flakes.[10a] These are likely to evolve from re-aggregation and concomitant folding of few-layer graphene flakes. Most of the flake sizes range from 1 to 2 μm^2 with some of them exceeding 5 μm^2. It has to be noted here that the surfaces of the flakes (Figure 3 and S5), irrespective of **2** or **3**, carry an amorphous coating, which cannot exclusively be explained by the functionalization. Next to functional groups, solvent residues cannot be entirely ruled out despite the thorough and multistep cleaning procedure.

Additional information about structural and electronic features were derived from Raman experiments with drop

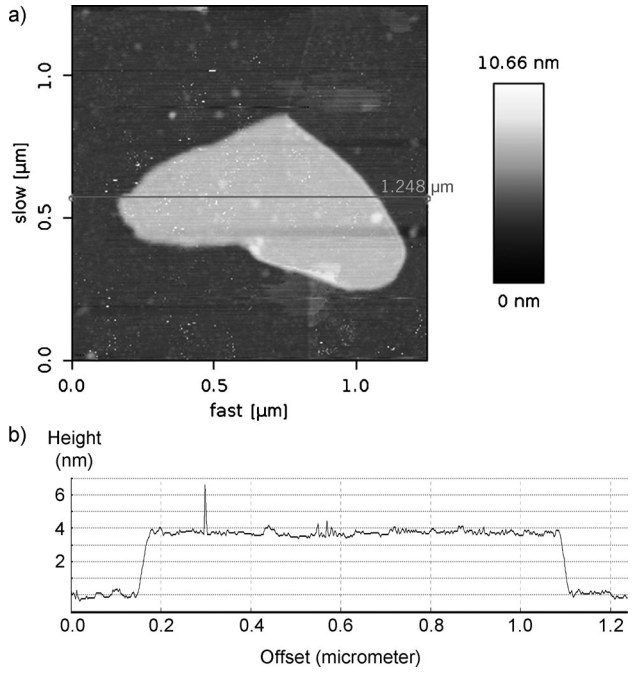

Figure 2. a) Tapping mode AFM image of **3** on a mica surface. b) The corresponding height profile taken along the grey line shown in (a). The sample was prepared by drop-casting a dilute dispersion of **3** in ethanol.

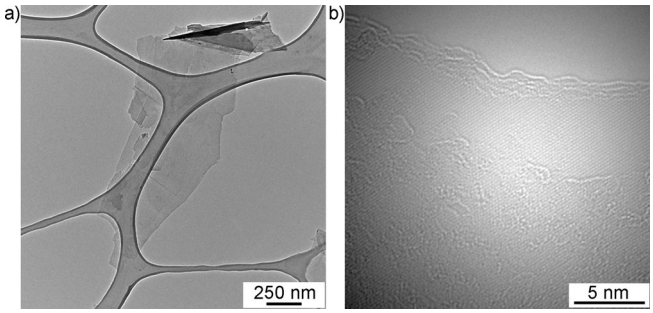

Figure 3. Bright-field TEM (a) and HRTEM (b) images of **3** drop casted from a DMF dispersion onto a lacey carbon grid.

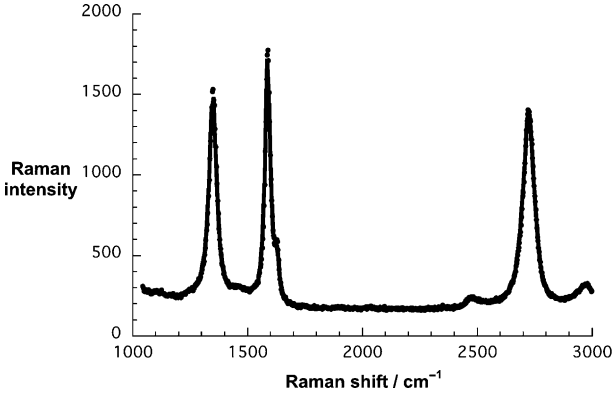

Figure 4. Raman spectrum of **3** drop casted from a DMF dispersion onto silicon oxide wafer and excited at $\lambda = 532$ nm.

casted DMF dispersions of **2** and **3** (see Figure S6 in the Supporting Information and Figure 4, respectively). Silicon wafers used were covered with a 300 nm thick oxide layer. Excitation of **3** at $\lambda = 532$ nm gives rise to the typical Raman peaks of exfoliated graphite, namely the D-band at 1351 cm^{-1}, the G-band at 1589 cm^{-1}, and a single maximum for the 2D-band at 2722 cm^{-1}. Upon exfoliation and functionalization, the D-band intensity increases (Figure S6). For both **2** and graphite dispersed in NMP, the Raman spectra show a symmetric 2D-band with full width at half maximum (FWHM) values of 86 cm^{-1} but a very small 2D/G ratio of 0.4, thus indicating the exfoliated nature of the materials with an increased turbostratic structure. Interestingly, the Raman spectrum of **3** shows a strong D-band. Responsible for this trend is, on one hand, the functionalization of the basal plane of graphene to form sp^3 domains and, on the other hand, a decreased flake size with stronger edge contribution to the double resonant Raman processes. The 2D-band is highly symmetric and is fitted by a single Lorentzian with a FWHM of 57 cm^{-1} and exhibits a 2D/G ratio of 0.9. The latter attests to the presence of graphite, which has been strongly exfoliated into few-layer graphene. Evidence for the electronic communication in graphene–Pc derives from resonantly exciting **3** at $\lambda = 633$ nm (Figure S7). Notably, the detection of any appreciable Raman spectrum is only possible because of the completely quenched Pc fluorescence (see below). A series of new Raman peaks arise in addition to the characteristic graphene peaks (see above) and the most dominant peaks are seen at 1562, 1497, 1409, 1314, and 1187 cm^{-1}. Correlating the Raman peaks with those known for **1** corroborates the successful functionalization of graphene with Pcs (Figure S8). It is reassuring that in reference experiments, in which **2** was excited at $\lambda = 633$ nm, none of the aforementioned Raman peaks were observed (Figure S7).

The ground-state features of Pcs in graphene–Pc **3** were probed by steady-state absorption experiments with freshly prepared dispersions in DMF by ultrasonication, not in excess of five minutes. In **3**, the typical Pc signatures appear as maxima at $\lambda = 673$ nm and at around $\lambda = 733$ nm.[17] Only the former correlates, however, with the Q-band absorption seen in **1** (Figure 5). The Soret-band transitions in the range between $\lambda = 300$ and 500 nm are superimposed, in the case of **3**, onto features which correspond to graphene absorptions

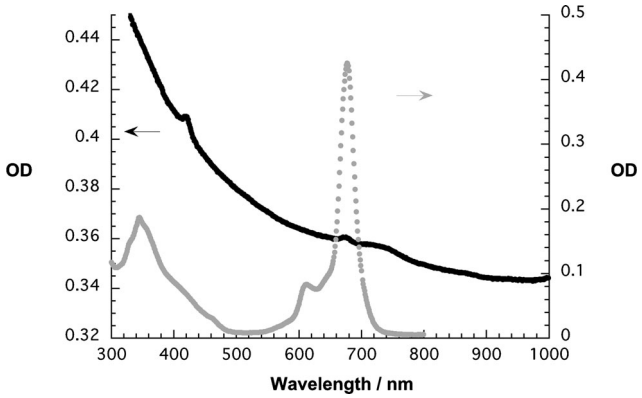

Figure 5. Absorption spectra of **1** (grey) and **3** (black) in DMF.

and light scattering. Importantly, the features (i.e., Q-and Soret-bands) appear strongly broadened and, most notably, are bathochromically shifted with respect to **1**. As a matter of fact, we take this as additional evidence in favor of strong electronic interactions between Pcs and the basal plane of graphene.[18] Solution behavior rather than light scattering was confirmed by performing a series of dilution experiments. In this context, linear relationships between the uniform dilution steps and the resulting decrease in optical density are in perfect agreement with the Lambert–Beer law. The absorption spectrum of **2** is, however, featureless and is best described as a monotonically decreasing absorption.

In complementary fluorescence assays, emphasis was placed on the fluorescent nature of Pc **1**, having a fluorescence maximum at $\lambda = 681$ nm, fluorescence quantum yields of 0.2, and fluorescence lifetimes of 4.6 ns (67 %; see Figure S9 in the Supporting Information). As a consequence of covalently linking **1** to the basal plane of graphene, no appreciable Pc fluorescence was noted for **3** in neither steady-state nor time-resolved experiments.

To gain insights into the product of fluorescence quenching, we employed femtosecond transient absorption measurements following excitation of dispersions of **1**, **2** and **3** at $\lambda =$ 387 nm in either NMP or DMF. In reference experiments with **1**, the instantaneous formation of the Pc singlet excited state is discernable throughout the visible and near-infrared section of the solar spectrum (see Figure S10 in the Supporting Information). Spectral attributes of the Pc singlet excited transient are minima around $\lambda = 610$ and 675 nm, which are good reflections of the ground-state bleaching, and maxima at $\lambda = 475$, 815, and 1025 nm. These features are metastable and decay rather slowly via intersystem crossing [i.e., (2.3 ± 0.5) ns] to the energetically lower lying triplet excited state. Most notable is a maximum for the latter at $\lambda = 500$ nm. A quantum yield of approximately 70 % has been derived for the triplet formation. The latter is oxygen sensitive and forms singlet oxygen with nearly diffusion controlled rate constants. In the absence of molecular oxygen the lifetime of the Pc triplet excited state is approximately 100 μs.

In complementary reference experiments with **2** in NMP, we note that upon excitation at $\lambda = 387$ nm, there is instantaneous bleaching [i.e., (0.5 ± 0.1) ps] of graphene-centered transitions in the range from $\lambda = 900$ to 1200 nm (see Figure S11 in the Supporting Information). For the major decay component of this bleaching, we determined a lifetime of (1.9 ± 0.5) ps corresponding to the reinstatement of the graphene ground state. Finally, turning to **3**, the rapid formation and deactivation of the singlet excited state characteristics of Pcs is discernable within a time window of 5 ps (Figure 6 and Figure S12). In particular, the spectral range for the Pc-centered bleaching extends from $\lambda = 500$ to 800 nm with distinct features at $\lambda = 650$, 735, and 770 nm which resemble those of the ground state. Simultaneously with the Pc singlet excited state decay, the formation of a new transient species evolves with maxima at $\lambda = 515$ and 850 nm which relate to the one-electron oxidized Pc. Similarly, the range beyond $\lambda = 1000$ nm (i.e., $\lambda = 1000$–1400 nm) is important, and is dominated by a broad bleaching immediately after the photoexcitation. Here, new features were noted during

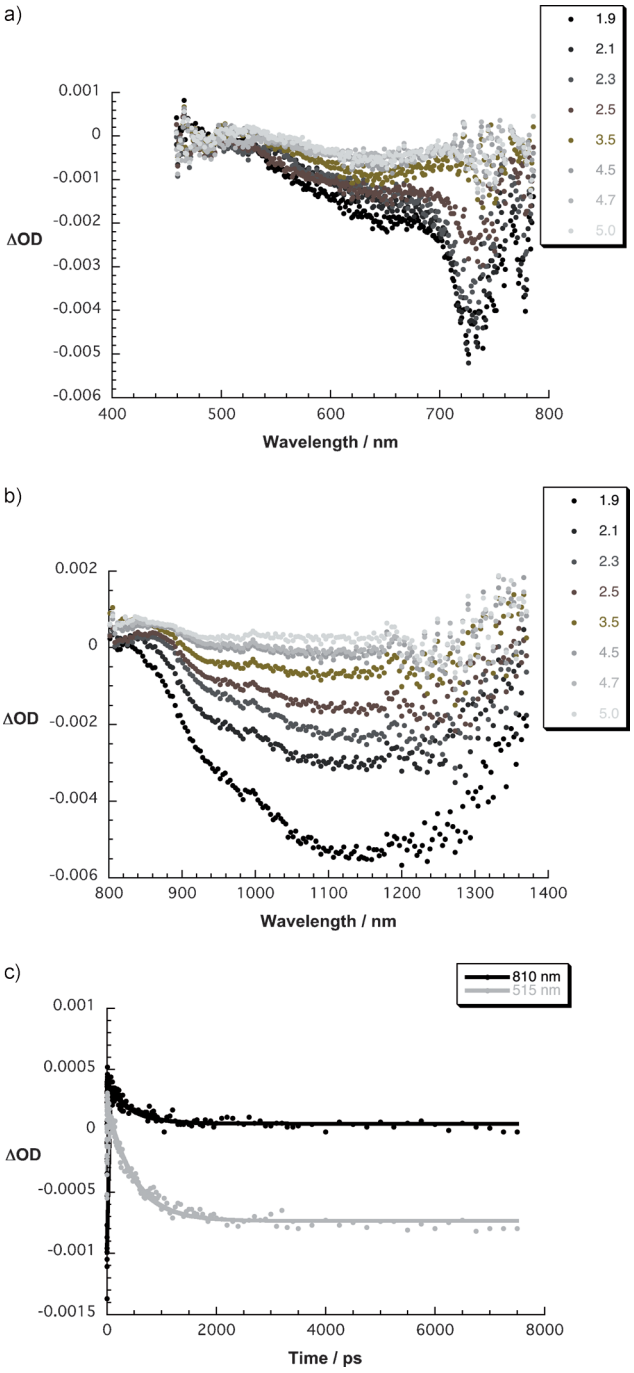

Figure 6. a) Differential absorption spectra (visible) of **3** in DMF, obtained upon femtosecond pump probe experiments ($\lambda = 387$ nm) with several time delays, between 1.9 and 5.0 ps (see legend), at room temperature. b) Differential absorption spectra (near-infrared) of **3** in DMF, obtained upon femtosecond pump probe experiments ($\lambda = 387$ nm) with several time delays, between 1.9 and 5.0 ps at room temperature. c) Time absorption profiles of the spectra at $\lambda = 515$ (grey) and 810 nm (black) showing the charge separation and charge recombination dynamics.

the transient decay with a broad maximum at $\lambda = 1100$ nm. Implicit are new conduction band electrons in graphene—injected from the photoexcited Pc. A multiwavelength analysis affords a short-lived and a long-lived component

with lifetimes of (3.3 ± 0.5) and (270 ± 10) ps, respectively, in DMF. Slightly longer is the lifetime in NMP at (340 ± 10) ps. In line with the aforementioned features we rationalize the kinetics in terms of charge separation and charge recombination.

To sum up, we present herein the first comprehensive investigation regarding the covalent attachment of a light harvester/electron donor, that is, a phthalocyanine, to the basal plane of few-layer graphene, on one hand, and its full-fledged physicochemical characterization, on the other hand. Most importantly, the latter includes the unambiguous corroboration by means of several steady-state and time-resolved assays of an ultrafast charge separation followed by a slower charge recombination.

Received: February 21, 2012
Revised: April 9, 2012
Published online: May 16, 2012

Keywords: electron transfer · energy conversion · graphene · photochemistry · phthalocyanines

[1] a) A. K. Geim, K. S. Novoselov, *Nat. Mater.* **2007**, *6*, 183; b) C. N. R. Rao, A. K. Sood, K. S. Subrahmanyam, A. Govindaraj, *Angew. Chem.* **2009**, *121*, 7890; *Angew. Chem. Int. Ed.* **2009**, *48*, 7752; c) M. J. Allen, V. C. Tung, R. B. Kaner, *Chem. Rev.* **2010**, *110*, 132; d) Z. Sun, D. K. James, J. M. Tour, *J. Phys. Chem. Lett.* **2011**, *2*, 2425.

[2] K. S. Novoselov, A. K. Geim, S. V. Morozov, D. Jiang, Y. Zhang, S. V. Dubonos, I. V. Grigorieva, A. A. Firsov, *Science* **2004**, *306*, 666.

[3] X. Huang, Z. Yin, S. Wu, X. Qi, Q. He, Q. Zhang, Q. Yan, F. Boey, H. Zhang, *Small* **2011**, *7*, 1876.

[4] D. M. Guldi, V. Sgobba, *Chem. Commun.* **2011**, *47*, 606.

[5] a) X. Wang, L. Zhi, K. Müllen, *Nano Lett.* **2008**, *8*, 323; b) G. Eda, G. Fanchini, M. Chhowalla, *Nat. Nanotechnol.* **2008**, *3*, 270.

[6] Z. Liu, Q. Liu, Y. Huang, Y. Ma, S. Yin, X. Zhang, W. Sun, Y. Chen, *Adv. Mater.* **2008**, *20*, 3924.

[7] a) X. Zhang, L. Hou, A. Cnossen, A. C. Coleman, O. Ivashenko, P. Rudolf, B. J. van Wees, W. R. Browne, B. L. Feringa, *Chem. Eur. J.* **2011**, *17*, 8957; b) H.-X. Wang, K.-G. Zhou, Y.-L. Xie, J. Zeng, N.-N. Chai, J. Li, H.-L. Zhang, *Chem. Commun.* **2011**, *47*, 5747; c) J. Geng, B.-S. Kong, S. B. Yang, H. T. Jung, *Chem. Commun.* **2010**, *46*, 5091; d) N. Karousis, A. S. D. Sandanayaka, T. Hasobe, S. P. Economopoulos, E. Sarantopoulou, N. Tagmatarchis, *J. Mater. Chem.* **2011**, *21*, 109; e) T. Umeyama, J. Mihara, N. Tezuka, Y. Matano, K. Stranius, V. Chukharev, N. V. Tkachenko, H. Lemmetyinen, K. Noda, K. Matsushige, T. Shishido, Z. Liu, K. Hirose-Takai, K. Suenaga, H. Imahori, *Chem. Eur. J.* **2012**, *18*, 4250.

[8] a) *The Porphyrin Handbook*, *Vol. 15–20* (Eds.: K. M. Kadish, K. M. Smith, R. Guilard), Academic Press, San Diego, **2003**; b) G. de la Torre, C. G. Claessens, T. Torres, *Chem. Commun.* **2007**, 2000; c) M. V. Martínez-Díaz, G. de la Torre, T. Torres, *Chem. Commun.* **2010**, *46*, 7090; d) G. Bottari, G. de la Torre, D. M. Guldi, T. Torres, *Chem. Rev.* **2010**, *110*, 6768.

[9] a) M. Castelaín, H. J. Salavagione, R. Gómez, J. L. Segura, *Chem. Commun.* **2011**, *47*, 7677; b) H. Bai, Y. Xu, L. Zhao, C. Li, G. Shi, *Chem. Commun.* **2009**, 1667; c) S. Stankovich, R. D. Piner, X. Q. Chem, N. Q. Wu, S. T. Nguyen, R. S. Ruoff, *J. Mater. Chem.* **2006**, *16*, 155; d) X. Qi, K.-Y. Pu, H. Li, X. Zhou, S. Wu, Q.-L. Fan, B. Liu, F. Boey, W. Huang, H. Zhang, *Angew. Chem.* **2010**, *122*, 9616; *Angew. Chem. Int. Ed.* **2010**, *49*, 9426; e) S. Barja, M. Garnica, J. J. Hinarejos, A. L. Vázquez de Parga, N. Martín, R. Miranda, *Chem. Commun.* **2010**, *46*, 8198.

[10] a) J. M. Englert, C. Dotzer, G. Yang, M. Schmid, C. Papp, J. M. Gottfried, H.-P. Steinrück, E. Spiecker, F. Hauke, A. Hirsch, *Nat. Chem.* **2011**, *3*, 279; b) M. Quintana, A. Montellano, A. E. del Rio Castillo, G. Van Tendeloo, C. Bittencourt, M. Prato, *Chem. Commun.* **2011**, *47*, 9330; c) M. Quintana, K. Spyrou, M. Grzelczak, W. R. Browne, P. Rudolf, M. Prato, *ACS Nano* **2010**, *4*, 3527; d) S. P. Economopoulos, G. Rotas, Y. Miyata, H. Shinohara, N. Tagmatarchis, *ACS Nano* **2010**, *4*, 7499.

[11] a) Y. Hernandez, V. Nicolosi, M. Lotya, F. M. Blighe, Z. Sun, S. De, I. T. McGovern, B. Holland, M. Byrne, Y. K. Gun'Ko, J. J. Boland, P. Niraj, G. Duesberg, S. Krishnamurthy, R. Goodhue, J. Hutchison, V. Scardaci, A. C. Ferrari, J. N. Coleman, *Nat. Nanotechnol.* **2008**, *3*, 563; b) U. Khan, A. O'Neill, M. Lotya, S. De, J. N. Coleman, *Small* **2010**, *6*, 864.

[12] a) A. Chunder, T. Pal, S. I. Khondaker, L. Zhai, *J. Phys. Chem. C* **2010**, *114*, 15129; b) X.-F. Zhang, Q. Xi, *Carbon* **2011**, *49*, 3842.

[13] J. Malig, N. Jux, D. Kiessling, J.-J. Cid, P. Vázquez, T. Torres, D. M. Guldi, *Angew. Chem.* **2011**, *123*, 3623; *Angew. Chem. Int. Ed.* **2011**, *50*, 3561.

[14] J. Zhu, Y. Li, Y. Chen, J. Wang, B. Zhang, J. Zhang, W. J. Blau, *Carbon* **2011**, *49*, 1900.

[15] B. Ballesteros, S. Campidelli, G. de la Torre, C. Ehli, D. M. Guldi, M. Prato, T. Torres, *Chem. Commun.* **2007**, 2950.

[16] V. Georgakilas, A. B. Bourlinos, R. Zboril, T. A. Steriotis, P. Dallas, A. K. Stubos, C. Trapalis, *Chem. Commun.* **2010**, *46*, 1766.

[17] Please note that in DMF solution Pcs usually show only one Q-band. See for example: J. Bartelmess, B. Ballesteros, G. de la Torre, D. Kiessling, S. Campidelli, M. Prato, T. Torres, D. M. Guldi, *J. Am. Chem. Soc.* **2010**, *132*, 16202.

[18] In light of the low concentration of Pcs, through space interactions are most likely to govern the electron-transfer communication between the graphene and Pc in **3**.

